Majorana stripe order on the surface of a three-dimensional topological insulator

Y. Kamiya,[1,*] A. Furusaki,[1] J. C. Y. Teo,[2] and G.-W. Chern[2,†]

[1]*Condensed Matter Theory Laboratory, RIKEN, Wako, Saitama 351-0198, Japan*
[2]*Department of Physics, University of Virginia, Charlottesville, Virginia 22904, USA*

The issue on the effect of interactions in topological states concerns not only interacting topological phases but also novel symmetry-breaking phases and phase transitions. Here we study the interaction effect on Majorana zero modes (MZMs) bound to a square vortex lattice in two-dimensional topological superconductors. Under the neutrality condition, where single-body hybridization between MZMs is prohibited by an emergent symmetry, a minimal square-lattice model for MZMs can be faithfully mapped to a quantum spin model, which has no sign problem in the world-line quantum Monte Carlo simulation. Guided by an insight from a further duality mapping, we demonstrate that the interaction induces a *Majorana stripe state*, a gapped state spontaneously breaking lattice translational and rotational symmetries, as opposed to the previously conjectured topological quantum criticality. Away from neutrality, a mean-field theory suggests a quantum critical point induced by hybridization.

Topological states are currently the focus of intensive research [1–3]. In particular, bulk-boundary correspondence is a central guiding principle, which predicts low-energy modes at the interface between topologically distinct states. It also applies to topological defects (such as dislocations and superconducting vortices) in topological matter, because they can be regarded as generalized interfaces bordering on normal states [4–11]. Of particular interest are Majorana zero modes (MZMs) at vortices in two-dimensional (2D) topological superconductors. Besides exploring the potential of MZMs for quantum computation [12–21], the idea of designing lattices of Majorana fermions out of MZMs is fascinating in its own right, because the interaction between MZMs may lead to novel phases and critical phenomena [22–30].

In this Rapid Communication, we study a square lattice of interacting MZMs, which may emerge at vortices in a 2D topological superfluid and superconductor [31–36], as predicted for the *A* phase of ^{3}He and Sr$_2$RuO$_4$ [37–39]. For definiteness, we consider a surface of a 3D strong topological insulator subject to superconducting proximity effect, as proposed by Fu and Kane [15]. The predicted surface state resembles a spinless $p_x \pm ip_y$ superconductor; see Refs. [40,41] for recent experimental progress. When an Abrikosov vortex lattice is induced by a magnetic field, MZMs are expected to emerge at vortices [5], leading to a lattice of Majorana fermions at low energies. Here we assume additional conditions to stabilize a square vortex lattice such as strong fourfold lattice anisotropy, which is less common than a triangular lattice but possible (e.g., LuNi$_2$B$_2$C [42]). We demonstrate that a faithful spin representation of a minimal interacting Hamiltonian for Majorana fermions can be derived in the

square lattice under the neutrality condition, which furthermore allows for employing a quantum Monte Carlo (QMC) method [43] to investigate thermodynamic properties of very large lattices unbiasedly. We find a *Majorana stripe phase* and present a duality transformation elucidating the nature of this phase, which supersedes the previously proposed topological quantum criticality [25]. We then extend our analysis away from neutrality by a mean-field (MF) theory by including the nearest-neighbor hybridization, where we find a quantum critical point induced by Majorana hybridization, beyond which Majorana fermions have gapless dispersion.

At the noninteracting level, the system is described in the long-wavelength limit by the Fu-Kane Hamiltonian [15] $\hat{H}_{\mathrm{FK}} = \frac{1}{2} \int d^2\mathbf{r} \, \hat{\Psi}_\mathbf{r}^\dagger \mathcal{H}_{\mathrm{FK}}(\mathbf{r}) \hat{\Psi}_\mathbf{r}$, with $\hat{\Psi}_\mathbf{r} = (\hat{\psi}_{\uparrow\mathbf{r}}, \hat{\psi}_{\downarrow\mathbf{r}}, \hat{\psi}_{\downarrow\mathbf{r}}^\dagger, -\hat{\psi}_{\uparrow\mathbf{r}}^\dagger)^{\mathrm{T}}$ being the Nambu spinor of the electronic operators $\hat{\psi}_{\alpha\mathbf{r}}^{(\dagger)}$ ($\alpha = \uparrow, \downarrow$) and

$$\mathcal{H}_{\mathrm{FK}}(\mathbf{r}) = \tau^z(-iv_{\mathrm{F}}\boldsymbol{\sigma} \cdot \nabla - \mu_{\mathrm{F}}) + \mathrm{Re}\,\Delta(\mathbf{r})\tau^x + \mathrm{Im}\,\Delta(\mathbf{r})\tau^y, \tag{1}$$

where σ (τ) is the Pauli matrix in the spin (Nambu) basis, μ_{F} is the chemical potential, $\Delta(\mathbf{r})$ is the proximity-induced pair potential, and v_{F} is velocity of the surface Dirac mode when $\Delta = 0$. The distribution and structure of vortices are encoded in $\Delta(\mathbf{r})$. The neutrality condition corresponds to $\mu_{\mathrm{F}} = 0$, which has a significant consequence on the emergent symmetry of the effective Hamiltonian [25,26]. When satisfied, an artificial time-reversal symmetry $\Theta_{\mathrm{eff}} = \sigma^x \tau^x K$ (K is the complex conjugation) with $\Theta_{\mathrm{eff}}^2 = 1$ emerges in addition to the particle-hole symmetry $\Xi = \sigma^y \tau^y K$ inherent to the Bogoliubov–de Gennes formalism. The consequence is that the vortex-bound MZM takes the form $\hat{\gamma} = \hat{\gamma}^\dagger = \int d^2\mathbf{r}(u_\mathbf{r}\hat{\psi}_{\downarrow,\mathbf{r}} + u_\mathbf{r}^*\hat{\psi}_{\downarrow,\mathbf{r}}^\dagger)$, i.e., with the spin antiparallel to the magnetic field [26]. Because $\hat{\Theta}_{\mathrm{eff}} \hat{\gamma} \, \hat{\Theta}_{\mathrm{eff}}^{-1} = \hat{\gamma}$ and $\hat{\Theta}_{\mathrm{eff}}$ is antiunitary, single-body hybridization $i\hat{\gamma}_\mathbf{r}\hat{\gamma}_{\mathbf{r}'}$ is prohibited
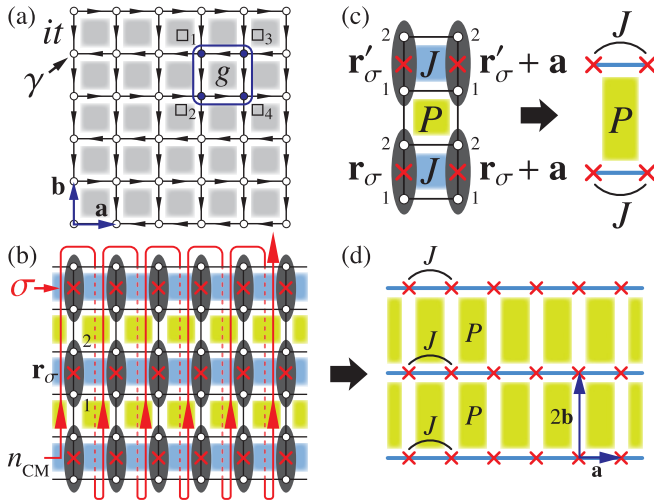
*yoshitomo.kamiya@riken.jp
†gchern@virginia.edu

FIG. 1. MZMs and the JW transformation. (a) Square lattice of MZM, where shaded plaquettes represent the interaction g and directed links from site $\mathbf{r}$ to site $\mathbf{r}'$ represent the hybridization term $it\hat{\gamma}_{\mathbf{r}}\hat{\gamma}_{\mathbf{r}'}$. (b) JW transformation of $\hat{H}_g$ with the column-major site ordering n_{CM}. Ellipses show pairing of MZMs with crosses representing σ spins. (c) A plaquette term involving two (four) pairs is transformed to the Ising (four-spin) coupling, where $\mathbf{r}'_{\sigma} = \mathbf{r}_{\sigma} + 2\mathbf{b}$. (d) Lattice of σ spins.

between any pair of MZMs at $\mathbf{r}$ and $\mathbf{r}'$. For an interacting many-body system, this means that the neutrality condition corresponds to the strong-coupling limit for the Majorana modes.

Assuming the simplest, quartic local interaction of the vortex Majorana modes on the square lattice, we consider the following Hamiltonian $\hat{H} = \hat{H}_g$ [25,28] with

$$\hat{H}_g = g \sum_{\square} \hat{\gamma}_{\square_1} \hat{\gamma}_{\square_2} \hat{\gamma}_{\square_3} \hat{\gamma}_{\square_4}, \qquad (2)$$

where $\hat{\gamma}_{\mathbf{r}}$ is the Majorana fermion operator at site $\mathbf{r}$ satisfying $\hat{\gamma}_{\mathbf{r}}^{\dagger} = \hat{\gamma}_{\mathbf{r}}$ and $\{\hat{\gamma}_{\mathbf{r}}, \hat{\gamma}_{\mathbf{r}'}\} = 2\delta_{\mathbf{r},\mathbf{r}'}$ and the summation runs over elementary plaquettes; $\square_1 - \square_4$ are four corners of a plaquette, $\square_2 = \square_1 - \mathbf{b}$, $\square_3 = \square_1 + \mathbf{a}$, and $\square_4 = \square_3 - \mathbf{b}$, with $\mathbf{a}$ and $\mathbf{b}$ the primitive lattice vectors [Fig. 1(a)].

As the hybridization term allowed for $\mu_{\mathrm{F}} \neq 0$ [44], we consider the following nearest-neighbor hybridization, discussed in, e.g., Refs. [25,34]:

$$\hat{H}_t = it \sum_{\mathbf{r}} [\hat{\gamma}_{\mathbf{r}} \hat{\gamma}_{\mathbf{r}-\mathbf{b}} + (-1)^{r_y} \hat{\gamma}_{\mathbf{r}} \hat{\gamma}_{\mathbf{r}+\mathbf{a}}], \qquad (3)$$

which has a uniform π flux per plaquette because of the underlying vortices. Equation (3) preserves the full symmetry of the square lattice (e.g., the translation in the $\mathbf{b}$ direction is accompanied by a gauge transformation). By continuity, we expect $|t| \ll |g|$ for small μ_{F}. We assume $g, t > 0$ unless otherwise mentioned.

We start from $\hat{H} = \hat{H}_g$ (2). Assuming a periodic (open) boundary condition in the $\mathbf{a}$ ($\mathbf{b}$) direction, we map it to a spin model by using a 2D Jordan-Wigner (JW) transformation. We define a complex fermion $\hat{c}_{\mathbf{r}_{\sigma}} = \frac{1}{2}(\hat{\gamma}_{\mathbf{r}_{\sigma},1} + i\hat{\gamma}_{\mathbf{r}_{\sigma},2})$ by introducing an artificial (but arbitrary) pairing convention [Fig. 1(b)], where $\mathbf{r}_{\sigma}$ is the position of a pair combining $\hat{\gamma}_{\mathbf{r}_{\sigma},1}$

and $\hat{\gamma}_{\mathbf{r}_{\sigma},2}$. Assuming the site-ordering ("column-major") index $n_{\mathrm{CM}}(\mathbf{r}_{\sigma})$ in Fig. 1(b), the transformation is $\hat{c}_{\mathbf{r}_{\sigma}}^{\dagger}\hat{c}_{\mathbf{r}_{\sigma}} = \frac{1}{2}(1 + \hat{\sigma}_{\mathbf{r}_{\sigma}}^z)$ and $\hat{c}_{\mathbf{r}_{\sigma}}^{\dagger} = \frac{1}{2}(\prod_{n_{\mathrm{CM}}(\mathbf{r}'_{\sigma}) < n_{\mathrm{CM}}(\mathbf{r}_{\sigma})} \hat{\sigma}_{\mathbf{r}'_{\sigma}}^z)(\hat{\sigma}_{\mathbf{r}_{\sigma}}^x + i\hat{\sigma}_{\mathbf{r}_{\sigma}}^y)$, where $\hat{\sigma}^{\alpha}$ ($\alpha = x, y, z$) are Pauli matrices. We find

$$\hat{\gamma}_{\mathbf{r}_{\sigma},2}\hat{\gamma}_{\mathbf{r}_{\sigma},1}\hat{\gamma}_{\mathbf{r}+\mathbf{a},2}\hat{\gamma}_{\mathbf{r}+\mathbf{a},1} = -\hat{\sigma}_{\mathbf{r}_1}^z \hat{\sigma}_{\mathbf{r}_1+\mathbf{a}}^z,$$

$$\hat{\gamma}_{\mathbf{r}'_{\sigma},1}\hat{\gamma}_{\mathbf{r}_{\sigma},2}\hat{\gamma}_{\mathbf{r}'_{\sigma}+\mathbf{a},1}\hat{\gamma}_{\mathbf{r}_{\sigma}+\mathbf{a},2} = -\hat{\sigma}_{\mathbf{r}_{\sigma}}^x \hat{\sigma}_{\mathbf{r}'_{\sigma}}^x \hat{\sigma}_{\mathbf{r}_{\sigma}+\mathbf{a}}^x \hat{\sigma}_{\mathbf{r}'_{\sigma}+\mathbf{a}}^x, \qquad (4)$$

with $\mathbf{r}'_{\sigma} = \mathbf{r}_{\sigma} + 2\mathbf{b}$, where the number of pairs involved in the interaction is two and four, respectively [Fig. 1(c)]. The string factor does not appear in either case. We obtain

$$\hat{H}_{g,\sigma} = -J \sum_{\mathbf{r}_{\sigma}} \hat{\sigma}_{\mathbf{r}_{\sigma}}^z \hat{\sigma}_{\mathbf{r}_{\sigma}+\mathbf{a}}^z - P \sum_{\square_{\sigma}} \left(\prod_{\mathbf{r}_{\sigma} \in \square_{\sigma}} \hat{\sigma}_{\mathbf{r}_{\sigma}}^x \right), \qquad (5)$$

with $J = P = g$, which combines the Ising coupling J on the horizontal bonds and a transverse four-spin term P associated with plaquettes ($\square_{\sigma}$) of σ spins [Fig. 1(b)]. In this representation (5), we can apply the world-line QMC method [43] to study the thermodynamic properties of MZMs without a negative sign problem. Specifically, we use the directed-loop algorithm [45,46] in the σ^x basis. To reduce finite-size effects, we use a trick of fictitious MZMs to simulate the lattice of Majorana fermions comprising an even number of plaquettes in the $\mathbf{b}$ direction (see Supplemental Material [47]). We investigate the spin lattices of $L \times L$ up to $L = 60$, corresponding to $L \times (2L - 1)$ MZMs, significantly larger than the previous exact diagonalization (ED) study up to 4×15 MZMs [25].

Figure 2(a) shows the specific heat C. In addition to the broad peak around temperature $T \approx g$, it exhibits a size-dependent sharp anomaly at $T/g \approx 0.25$, indicating a finite-temperature transition. This observation points to a symmetry breaking phase at low T, which contradicts with the previous ED study, where by introducing a two-site modulation in g [equivalent to making $J \neq P$ in Eq. (5)], it was suggested that the system becomes gapless when the original translational and rotational symmetries are recovered (i.e., $J = P$) [25]. To clarify the nature of the low-T state, we first note that the string operator $\hat{O}_{\mathrm{h}}^{\mathrm{spin}}(y) = \prod_{r_{\sigma}^x} \hat{\sigma}_{\mathbf{r}_{\sigma}=(r_{\sigma}^x,y)}^x$ is a conserved quantity for any horizontal ($\parallel \mathbf{a}$) chain, which flips σ^z eigenvalues of all spins at $r_{\sigma}^y = y$. Known as a generalized Elitzur's theorem [48], the corresponding gaugelike 1D symmetries reduce the effective dimensionality of the order parameter field σ^z from 2D to 1D. Hence the conservation of $\hat{O}_{\mathrm{h}}^{\mathrm{spin}}(y)$ prohibits any kind of long-range order of σ^z at $T > 0$; this 1D physics may explain the broad peak of C at high T, but not the transition itself.

To elucidate the nature of the low-T phase and the transition, we show that $\hat{H}_{g,\sigma}$ (hence $\hat{H}_g$) is dual to decoupled two copies of a square-lattice quantum compass model (see Supplemental Material [47]). This model was investigated in depth in various contexts [49–60], and the corresponding knowledge is very useful for understanding the nature of the low-T phase. Explicitly, we first define "τ spins" at the midpoint of every horizontal link. With the "row-major" site ordering $n_{\mathrm{RM}}(\mathbf{r}_{\sigma})$ in Fig. 3(a), the first transformation is $\hat{\tau}_{\mathbf{r}_{\tau}}^z = \hat{\sigma}_{\mathbf{r}_{\sigma}}^z \hat{\sigma}_{\mathbf{r}_{\sigma}+\mathbf{a}}^z$, $\hat{\tau}_{\mathbf{r}_{\tau}}^x = \prod_{n_{\mathrm{RM}}(\mathbf{r}'_{\sigma}) \leqslant n_{\mathrm{RM}}(\mathbf{r}_{\sigma})} \hat{\sigma}_{\mathbf{r}'_{\sigma}}^x$ with $\mathbf{r}_{\tau} = \mathbf{r}_{\sigma} + \frac{\mathbf{a}}{2}$, by which the J and P terms become an effective magnetic
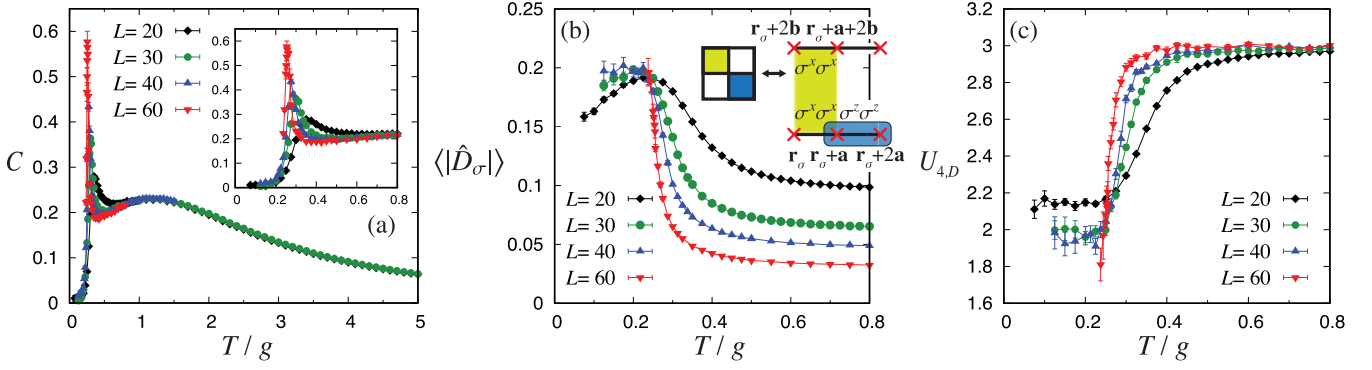
FIG. 2. QMC results in the spin representation (5) with $J = P = g$ in the $L \times L$ lattice with the fictitious MZM trick (see Supplemental Material [47]). (a) Specific heat $C = (1/L^2)\partial\langle\hat{H}_{g,\sigma}\rangle/\partial T$, (b) the order parameter $\langle|\hat{D}_\sigma|\rangle$ of the Majorana stripe state, and (c) the Binder parameter. The inset in (b) illustrates the local order parameter $\hat{D}_\sigma(\mathbf{r}_\sigma)$ (8) and its relation with a pair of Majorana plaquettes.

field and a four-spin interaction for τ spins, respectively. We find that the new four-spin interaction does not mix τ spins in even and odd columns, e.g., $\hat{\sigma}^x_{\mathbf{r}_\sigma}\hat{\sigma}^x_{\mathbf{r}_\sigma+\mathbf{a}}\hat{\sigma}^x_{\mathbf{r}_\sigma+2\mathbf{b}}\hat{\sigma}^x_{\mathbf{r}_\sigma+\mathbf{a}+2\mathbf{b}} = \hat{\tau}^x_{\mathbf{r}_\tau-\mathbf{a}}\hat{\tau}^x_{\mathbf{r}_\tau+\mathbf{a}}\hat{\tau}^x_{\mathbf{r}_\tau-\mathbf{a}+2\mathbf{b}}\hat{\tau}^x_{\mathbf{r}_\tau+\mathbf{a}+2\mathbf{b}}$ [Fig. 3(d)]. Consequently, the dual Hamiltonian is composed of decoupled even and odd components as $\hat{H}_{g,\tau} = \hat{H}^e_{g,\tau} + \hat{H}^o_{g,\tau}$, with

$$\hat{H}^{e(o)}_{g,\tau} = \sum_{\substack{\mathbf{r}_\tau \in \text{even} \\ \text{(odd) columns}}} \left(-J\hat{\tau}^z_{\mathbf{r}_\tau} - P\hat{\tau}^x_{\mathbf{r}_\tau}\hat{\tau}^x_{\mathbf{r}_\tau+2\mathbf{a}}\hat{\tau}^x_{\mathbf{r}_\tau+2\mathbf{b}}\hat{\tau}^x_{\mathbf{r}_\tau+2\mathbf{a}+2\mathbf{b}}\right).$$

(6)

To complete the mapping, we introduce "μ spins" at the midpoint of each vertical link ($\mathbf{r}_\tau, \mathbf{r}_\tau + 2\mathbf{b}$) for τ spins, such that $\hat{\mu}^x_{\mathbf{r}_\mu} = \hat{\tau}^x_{\mathbf{r}_\tau}\hat{\tau}^x_{\mathbf{r}_\tau+2\mathbf{b}}$, $\hat{\mu}^z_{\mathbf{r}_\mu} = \prod_{\tilde{n}_{\text{CM}}(\mathbf{r}'_\tau)\leqslant\tilde{n}_{\text{CM}}(\mathbf{r}_\tau)}\hat{\tau}^z_{\mathbf{r}_\tau}$ with $\mathbf{r}_\mu = \mathbf{r}_\tau + \mathbf{b}$, where $\tilde{n}_{\text{CM}}(\mathbf{r}_\tau)$ is the column-major ordering for τ spins [Fig. 3(b)]. This preserves the decoupling of $\hat{H}^e_{g,\tau}$ and $\hat{H}^o_{g,\tau}$,
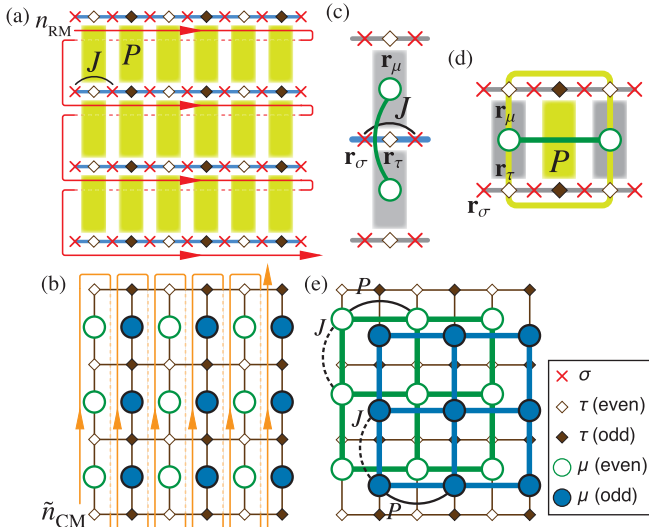

FIG. 3. Two-step duality transformation, introducing (a) τ spins and (b) μ spins. (c) The J term is transformed to the interaction $\hat{\mu}^z_{\mathbf{r}_\mu}\hat{\mu}^z_{\mathbf{r}_\mu+2\mathbf{b}}$. (d) The P term (highlighted filled rectangle) is transformed first into a four-spin coupling for τ spins (round rectangle) and then to $\hat{\mu}^x_{\mathbf{r}_\mu}\hat{\mu}^x_{\mathbf{r}_\mu+2\mathbf{a}}$. (e) Resulting decoupled copies of the quantum compass model for μ spins (shifted vertically for clarity).

transforming each into the quantum compass model on a square lattice with an enlarged unit cell [Figs. 3(c) and 3(e)],

$$\hat{H}^{e(o)}_{g,\mu} = \sum_{\mathbf{r}_\mu \in \text{even (odd) column}} \left(-P\hat{\mu}^x_{\mathbf{r}_\mu}\hat{\mu}^x_{\mathbf{r}_\mu+2\mathbf{a}} - J\hat{\mu}^z_{\mathbf{r}_\mu}\hat{\mu}^z_{\mathbf{r}_\mu+2\mathbf{b}}\right).$$

(7)

The total Hamiltonian is $\hat{H}_{g,\mu} = \hat{H}^e_{g,\mu} + \hat{H}^o_{g,\mu}$.

The most crucial input from the duality transformation is that the compass model with $J = P = g$ is known to undergo a "nematic" transition in the Ising universality class at a finite temperature [50,53,54]. Below the critical temperature $T = T_c$, the $\mathbb{Z}_2$ spin-lattice reflection symmetry [$x \leftrightarrow z$ ($\mathbf{a} \leftrightarrow \mathbf{b}$) in the spin (real) space] is spontaneously broken, while any spin-spin correlation function such as $\langle\hat{\mu}^x_{\mathbf{r}_\mu}\hat{\mu}^x_{\mathbf{r}'_\mu}\rangle$ and $\langle\hat{\mu}^z_{\mathbf{r}_\mu}\hat{\mu}^z_{\mathbf{r}'_\mu}\rangle$ remains short ranged. This $\mathbb{Z}_2$ symmetry breaking can be detected by a directional order parameter $\hat{D}_\mu(\mathbf{r}_\mu) = \hat{\mu}^x_{\mathbf{r}_\mu}\hat{\mu}^x_{\mathbf{r}_\mu+2\mathbf{a}} - \hat{\mu}^z_{\mathbf{r}_\mu}\hat{\mu}^z_{\mathbf{r}_\mu+2\mathbf{b}}$ [49]. Back to the language of Majorana fermions, the even-odd decomposition ($\hat{H}_{g,\mu} = \hat{H}^e_{g,\mu} + \hat{H}^o_{g,\mu}$) corresponds to the geometrical checkerboard decomposition of $\hat{H}_g$ (2). Defining $\hat{H}^A_g$ and $\hat{H}^B_g$ as composed of quartic interactions in one sublattice (A) of the checkerboard decomposition and its complement (B), respectively [Fig. 4(a)], we find $\hat{H}_g = \hat{H}^A_g + \hat{H}^B_g$ and $[\hat{H}^A_g, \hat{H}^B_g] = 0$. Here, $\hat{H}^A_g$ corresponds to $\hat{H}^e_{g,\mu}$ or $\hat{H}^o_{g,\mu}$ and $\hat{H}^B_g$ does to the other. In fact, each Ising-like bond interaction in $\hat{H}^{e(o)}_{g,\mu}$ (7) corresponds to a plaquette term that it graphically overlaps in the lattice, as illustrated in Fig. 4(a). Hence the nematic order quantified by $\hat{D}_\mu$ corresponds to a *spontaneous energy density modulation* associated with the plaquette interaction g. As shown in Fig. 4(b), the even-odd decoupling implies that the energy-density wave order emerges in the two sublattices A and B independently ($\mathbb{Z}_2 \times \mathbb{Z}_2$ symmetry breaking), resulting in fourfold degenerate ground states modulo the aforementioned 1D symmetries.

We confirm this Majorana stripe order by evaluating the order parameter by QMC. Figure 2(b) shows $\langle|\hat{D}_\sigma|\rangle$ with $\hat{D}_\sigma = \mathcal{N}^{-1}\sum'_{\mathbf{r}_\sigma}\hat{D}_\sigma(\mathbf{r}_\sigma)$, where the summation runs over either even or odd columns, $\mathcal{N}$ is a proper normalization (see Supplemental Material [47]), and

$$\hat{D}_\sigma(\mathbf{r}_\sigma) = \hat{\sigma}^z_{\mathbf{r}_\sigma+\mathbf{a}}\hat{\sigma}^z_{\mathbf{r}_\sigma+2\mathbf{a}} - \hat{\sigma}^x_{\mathbf{r}_\sigma+2\mathbf{b}}\hat{\sigma}^x_{\mathbf{r}_\sigma+\mathbf{a}+2\mathbf{b}}\hat{\sigma}^x_{\mathbf{r}_\sigma+\mathbf{a}}$$
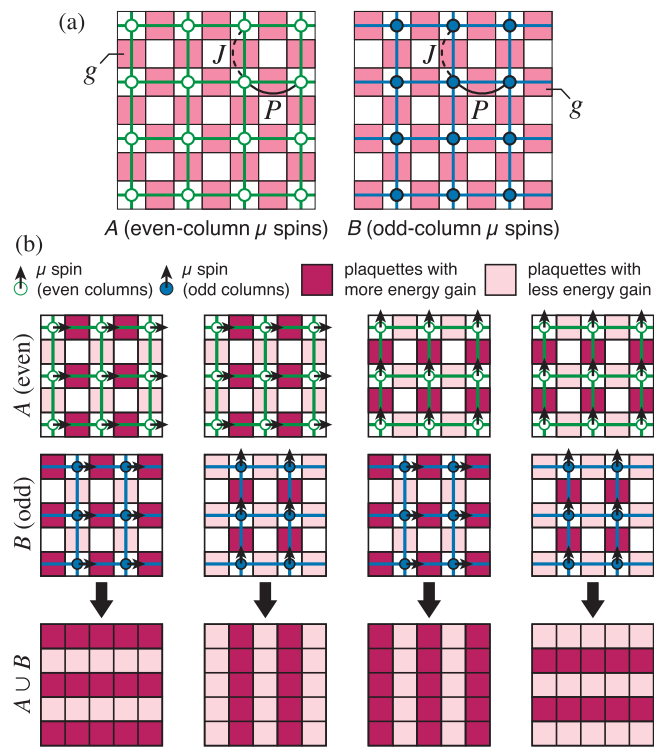
(8)

FIG. 4. Majorana stripe order. (a) Correspondence between the checkerboard decomposition of $\hat{H}_g$ (2) and the even and odd components of the compass model. (b) Fourfold degenerate ordered state and the relation with the nematic order in the compass model.

FIG. 5. MF results for $\hat{H}_t + \hat{H}_g$. (a) Schematic phase diagram in the T-Δg plane showing a first-order transition line ending at finite-T critical point. (b) Stripe order parameter D as a function of Δg for $t/g = 0.2, 0.8$. (c) Majorana MF band structure for varying t. (d) Energy gap $\varepsilon_{\text{gap}}(t)$ for $\Delta g = 0$, which is related to the jump ΔD of the stripe order parameter at $\Delta g = 0$ as $\varepsilon_{\text{gap}} = g\Delta D$ (see Supplemental Material [47]).

is the order parameter in the σ-spin representation. We find that the temperature dependence of $\langle |D| \rangle$ is consistent with the transition into the Majorana stripe phase (the nonmonotonic T dependence for small L is suggested to be a finite-size effect due to the open boundary condition in the **b** direction). Figure 2(c) shows the Binder parameter $U_{4,D} = \langle \hat{D}_\sigma^4 \rangle / \langle \hat{D}_\sigma^2 \rangle^2$, which exhibits crossing for different L, providing another confirmation of the transition. The crossing takes place at $T_c/g \approx 0.25(1)$, in agreement with the location of the divergent peak of C.

Finally, we consider the effect of the nearest-neighbor hybridization $\hat{H}_t$ (3) on the Majorana stripe phase. The finite-temperature Ising transition implies a first-order transition line in the extended T-Δg phase diagram [Fig. 5(a)], where nonzero $\Delta g \equiv P - J$ explicitly breaks the translational symmetry [Fig. 1(c)]. Since the QMC method has the sign problem when applied to $\hat{H} = \hat{H}_g + \hat{H}_t$, we employ the MF approximation in the Majorana representation to examine the discontinuous transition at $T = 0$. Figure 5(b) shows the order parameter $D = \langle \hat{D}_\sigma \rangle$ as a function of $\Delta g/g$ for $t/g = 0.2, 0.8$. For $t/g = 0.2$, D remains finite as $\Delta g \to 0$, and exhibits a jump upon changing the sign of Δg, indicating that the discontinuous transition persists even in the presence of weak hybridization. This in turn implies that the finite-T transition remains stable for small t, although the induced coupling between the A and B subsystems may alter the universality class [61]. As t increases, the discontinuity at $\Delta g = 0$, ΔD, is reduced and vanishes for $t > t_c \approx 0.65g$ [Fig. 5(d)]. As shown in Fig. 5(c), the MF band structure of Majorana
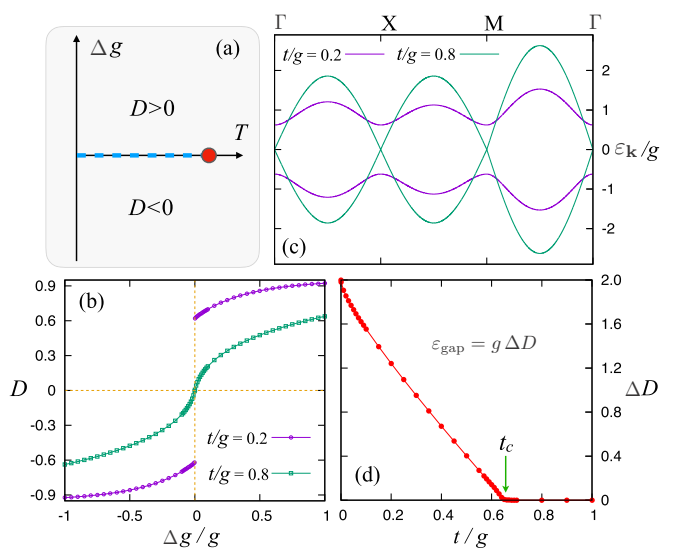
fermions in the limit $\Delta g \to 0$ in the stripe phase ($t < t_c$) is gapped with a topologically trivial band structure, where the energy gap is $\varepsilon_{\text{gap}} = g\Delta D$ (see Supplemental Material [47]). With increasing t, the gap reduces and vanishes for $t \geqslant t_c$, giving rise to a critical state with gapless Majorana fermions. Assuming that the critical temperature $T_c \approx \varepsilon_{\text{gap}}$, our result suggests $T_c \to 0$ as $t \to t_c$. Our calculation thus points to the existence of a quantum critical point characterized by gapless Majorana fermion excitations for $t \geqslant t_c$. We note that the effect of including second-neighbor hybridization, which produces a gap in the excitation spectrum, was recently discussed [28].

In summary, the square-lattice Majorana Hamiltonian $\hat{H}_t + \hat{H}_g$, which may have an experimental realization in the hybrid of a 3D strong topological insulator and a superconductor, induces a stripe order that spontaneously breaks the translational and rotational symmetries in the strong-coupling regime $g \gg t$, as opposed to the previously conjectured topological quantum critical behavior [25]. Our large-scale QMC simulation as well as the duality mapping (via the JW transformation) provide a solid confirmation of this phenomenon. We note that Affleck *et al.* also investigated the same model recently from the weak-coupling side, suggesting that the quantum phase transition $t = t_c$ belongs to a supersymmetric universality class [28]. Our unbiased approach coming from the strong coupling is complementary to their weak-coupling analysis. In fact, $t \neq 0$ lifts the 1D gaugelike symmetries, reducing the Majorana stripe state to the dimerized state found by Affleck *et al.* using a MF treatment similar to ours. We hope that our work will trigger an experimental effort in the search for intriguing phase transitions in the system of interacting Majorana modes, which may be synthesized on the surface of a 3D topological insulator as proposed recently [25,26].

[1] M. Z. Hasan and C. L. Kane, Rev. Mod. Phys. **82**, 3045 (2010).

[2] X.-L. Qi and S.-C. Zhang, Rev. Mod. Phys. **83**, 1057 (2011).

[3] C.-K. Chiu, J. C. Y. Teo, A. P. Schnyder, and S. Ryu, Rev. Mod. Phys. **88**, 035005 (2016).

[4] Y. Ran, Y. Zhang, and A. Vishwanath, Nat. Phys. **5**, 298 (2009).

[5] J. C. Y. Teo and C. L. Kane, Phys. Rev. B **82**, 115120 (2010).

[6] V. Juričić, A. Mesaros, R.-J. Slager, and J. Zaanen, Phys. Rev. Lett. **108**, 106403 (2012).

[7] R.-J. Slager, A. Mesaros, V. Juričić, and J. Zaanen, Nat. Phys. **9**, 98 (2012).

[8] T. L. Hughes, H. Yao, and X.-L. Qi, Phys. Rev. B **90**, 235123 (2014).

[9] J. C. Y. Teo and T. L. Hughes, Phys. Rev. Lett. **111**, 047006 (2013).

[10] R.-J. Slager, A. Mesaros, V. Juričić, and J. Zaanen, Phys. Rev. B **90**, 241403 (2014).

[11] J. C. Teo and T. L. Hughes, Annu. Rev. Condens. Matter Phys. **8**, 211 (2017).

[12] A. Kitaev, Ann. Phys. (NY) **303**, 2 (2003).

[13] C. Nayak, S. H. Simon, A. Stern, M. Freedman, and S. Das Sarma, Rev. Mod. Phys. **80**, 1083 (2008).

[14] A. Kitaev, Ann. Phys. (NY) **321**, 2 (2006).

[15] L. Fu and C. L. Kane, Phys. Rev. Lett. **100**, 096407 (2008).

[16] C. W. J. Beenakker, Annu. Rev. Condens. Matter Phys. **4**, 113 (2013).

[17] J. Alicea, Rep. Prog. Phys. **75**, 076501 (2012).

[18] T. D. Stanescu and S. Tewari, J. Phys.: Condens. Matter **25**, 233201 (2013).

[19] M. Leijnse and K. Flensberg, Semicond. Sci. Technol. **27**, 124003 (2012).

[20] S. R. Elliott and M. Franz, Rev. Mod. Phys. **87**, 137 (2015).

[21] S. Das Sarma, M. Freedman, and C. Nayak, npj Quantum Inf. **1**, 15001 (2015).

[22] A. Rahmani, X. Zhu, M. Franz, and I. Affleck, Phys. Rev. Lett. **115**, 166401 (2015).

[23] A. Rahmani, X. Zhu, M. Franz, and I. Affleck, Phys. Rev. B **92**, 235123 (2015).

[24] A. Milsted, L. Seabra, I. C. Fulga, C. W. J. Beenakker, and E. Cobanera, Phys. Rev. B **92**, 085139 (2015).

[25] C.-K. Chiu, D. I. Pikulin, and M. Franz, Phys. Rev. B **91**, 165402 (2015).

[26] C.-K. Chiu, D. I. Pikulin, and M. Franz, Phys. Rev. B **92**, 241115 (2015).

[27] X. Zhu and M. Franz, Phys. Rev. B **93**, 195118 (2016).

[28] I. Affleck, A. Rahmani, and D. Pikulin, Phys. Rev. B **96**, 125121 (2017).

[29] T. Hayata and A. Yamamoto, Phys. Rev. B **96**, 035129 (2017).

[30] N. Sannomiya and H. Katsura, arXiv:1712.01148.

[31] G. E. Volovik, Pisma Zh. Eksp. Teor. Fiz. **70**, 601 (1999) [JETP Lett. **70**, 609 (1999)].

[32] N. Read and D. Green, Phys. Rev. B **61**, 10267 (2000).

[33] D. A. Ivanov, Phys. Rev. Lett. **86**, 268 (2001).

[34] E. Grosfeld and A. Stern, Phys. Rev. B **73**, 201303 (2006).

[35] C.-K. Chiu, P. Ghaemi, and T. L. Hughes, Phys. Rev. Lett. **109**, 237009 (2012).

[36] R. R. Biswas, Phys. Rev. Lett. **111**, 136401 (2013).

[37] S. Das Sarma, C. Nayak, and S. Tewari, Phys. Rev. B **73**, 220502 (2006).

[38] S. B. Chung, H. Bluhm, and E.-A. Kim, Phys. Rev. Lett. **99**, 197002 (2007).

[39] J. Jang, D. G. Ferguson, V. Vakaryuk, R. Budakian, S. B. Chung, P. M. Goldbart, and Y. Maeno, Science **331**, 186 (2011).

[40] J.-P. Xu, C. Liu, M.-X. Wang, J. Ge, Z.-L. Liu, X. Yang, Y. Chen, Y. Liu, Z.-A. Xu, C.-L. Gao, D. Qian, F.-C. Zhang, and J.-F. Jia, Phys. Rev. Lett. **112**, 217001 (2014).

[41] J.-P. Xu, M.-X. Wang, Z. L. Liu, J.-F. Ge, X. Yang, C. Liu, Z. A. Xu, D. Guan, C. L. Gao, D. Qian, Y. Liu, Q.-H. Wang, F.-C. Zhang, Q.-K. Xue, and J.-F. Jia, Phys. Rev. Lett. **114**, 017001 (2015).

[42] Y. De Wilde, M. Iavarone, U. Welp, V. Metlushko, A. E. Koshelev, I. Aranson, G. W. Crabtree, and P. C. Canfield, Phys. Rev. Lett. **78**, 4273 (1997).

[43] J. E. Gubernatis, N. Kawashima, and P. Werner, *Quantum Monte Carlo Methods* (Cambridge University Press, Cambridge, UK, 2016).

[44] M. Franz and Z. Tešanović, Phys. Rev. Lett. **84**, 554 (2000).

[45] O. F. Syljuåsen and A. W. Sandvik, Phys. Rev. E **66**, 046701 (2002).

[46] F. Alet, S. Wessel, and M. Troyer, Phys. Rev. E **71**, 036706 (2005).

[47] See Supplemental Material at http://link.aps.org/supplemental/10.1103/PhysRevB.98.161409 for details on the duality transformations, the fictitious MZM trick, and details of the MF calculation.

[48] C. D. Batista and Z. Nussinov, Phys. Rev. B **72**, 045137 (2005).

[49] Z. Nussinov and J. van den Brink, Rev. Mod. Phys. **87**, 1 (2015).

[50] A. Mishra, M. Ma, F.-C. Zhang, S. Guertler, L.-H. Tang, and S. Wan, Phys. Rev. Lett. **93**, 207201 (2004).

[51] J. Dorier, F. Becca, and F. Mila, Phys. Rev. B **72**, 024448 (2005).

[52] H.-D. Chen, C. Fang, J. Hu, and H. Yao, Phys. Rev. B **75**, 144401 (2007).

[53] T. Tanaka and S. Ishihara, Phys. Rev. Lett. **98**, 256402 (2007).

[54] S. Wenzel and W. Janke, Phys. Rev. B **78**, 064402 (2008).

[55] R. Orús, A. C. Doherty, and G. Vidal, Phys. Rev. Lett. **102**, 077203 (2009).

[56] C. Xu and J. E. Moore, Phys. Rev. Lett. **93**, 047003 (2004).

[57] C. Xu and J. Moore, Nucl. Phys. B **716**, 487 (2005).

[58] Z. Nussinov and E. Fradkin, Phys. Rev. B **71**, 195120 (2005).

[59] J. Vidal, R. Thomale, K. P. Schmidt, and S. Dusuel, Phys. Rev. B **80**, 081104 (2009).

[60] J. Nasu, Y. Kato, J. Yoshitake, Y. Kamiya, and Y. Motome, Phys. Rev. Lett. **118**, 137203 (2017).

[61] J. Ashkin and E. Teller, Phys. Rev. **64**, 178 (1943).